Biophysical Chemistry 203–204 (2015) 41–50

Contents lists available at ScienceDirect

Biophysical Chemistry

journal homepage: http://www.elsevier.com/locate/biophyschem

Non-two-state thermal denaturation of ferricytochrome *c* at neutral and slightly acidic pH values

Rastislav Varhač [a], Dagmar Sedláková [b], Marek Stupák [c], Erik Sedlák [a,d,*]

[a] Department of Biochemistry, P.J. Šafárik University, Moyzesova 11, 040 01 Košice, Slovakia
[b] Department of Biophysics, Institute of Experimental Physics Slovak Academy of Sciences, Watsonova 47, 040 01 Košice, Slovakia
[c] Department of Medical and Clinical Biochemistry, Faculty of Medicine, P.J. Šafárik University, Trieda SNP 1, 040 11 Košice, Slovakia
[d] Centre for Interdisciplinary Biosciences, P.J. Šafárik University, Jesenná 5, 040 01 Košice, Slovakia

HIGHLIGHTS

- Thermal denaturation of cyt *c* at pH > 5 has a non-two-state nature.
- Thermal transition of cyt *c* at pH > 5 proceeds through non-native low-spin states.
- Local conformational transition resembles alkaline-like transition.
- Final state of global conformational transition resembles bis-histidinyl state.
- Thermal transition of cyt *c* at pH < 5 is a one step process from low to high-spin states.

GRAPHICAL ABSTRACT

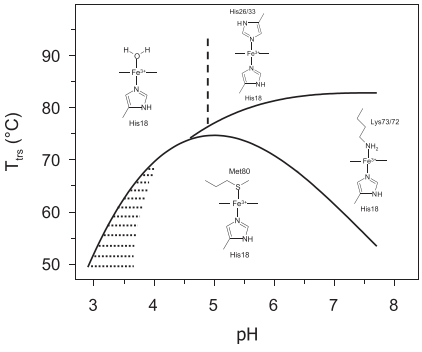

ARTICLE INFO

Article history:
Received 17 April 2015
Received in revised form 8 May 2015
Accepted 11 May 2015
Available online 19 May 2015

Keywords:
Protein stability
Conformational change
Ligand exchange
Alkaline state
Thermal denaturation

ABSTRACT

Thermal denaturation of ferricytochrome c (cyt c) has been methodically studied by absorbance, fluorescence, circular dichroism spectroscopy, viscosimetry and differential scanning calorimetry in pH range from pH 3.5 to 7.5. Thermal transitions have been monitored by intrinsic local probes of heme region such as absorbance at Soret, 620 nm and 695 nm bands and circular dichroism signals at 417 nm. Global conformational changes were analyzed by circular dichroism signal at 222 nm, fluorescence of the single tryptophan, reduced viscosity and differential scanning calorimetry. We show that cyt c thermal denaturation above pH ~5 can be described by an apparent two-step transition in which the heme iron stays in a low-spin state. The thermal denaturations of cyt c below pH ~5 proceed in one step to an unfolded highly compact form with a high-spin state of the heme iron. Cyt c conformational plasticity is discussed in regard to its physiological functions.

1. Introduction

Cytochrome *c* is a small globular protein consisting of a single polypeptide chain and a heme group covalently attached to it. In the native form, its heme iron is hexacoordinated, the fifth and sixth axial ligands being provided by the side chains of His18 and Met80, respectively [1]. In this configuration, the protein is in the low-spin state.

Abbreviations: cyt *c*, ferricytochrome *c*; GdnHCl, guanidine hydrochloride; CD, circular dichroism; DSC, differential scanning calorimetry.

* Corresponding author at: Centre for Interdisciplinary Biosciences, P.J. Šafárik University, Jesenná 5, 040 01 Košice, Slovakia.
E-mail address: erik.sedlak@upjs.sk (E. Sedlák).

http://dx.doi.org/10.1016/j.bpc.2015.05.002
0301-4622/

The pioneering work of Theorell and Åkesson [2] revealed five equilibrium conformers of ferricytochrome *c* (cyt *c*) over a conventional pH scale (0–14). Their findings pointed out that cyt *c*, besides its native functional form, can exist in at least one alternative conformation with low-spin state of heme iron at alkaline pH at room temperature — in the so-called alkaline state. The fact that modified properties (e.g. redox potential of the heme iron) of cyt *c* in the alkaline state might affect its physiological role in mitochondria has attracted a lot of interest in studying its properties. Intensive studies led to a finding that Met80 is in the alkaline state replaced by one of the lysine side chains (Lys72, Lys73 and Lys79) [3–7]. Interestingly, the critical roles of these lysines have been very recently implied also in cyt *c*–cardiolipin recognition and thus as well in peroxidase activity of cyt *c* in early steps of apoptosis [8,9].

Myer et al. [10] showed that chemical denaturation of cyt *c* is a complex process consistent with the mechanism: $N \leftrightarrows nX \leftrightarrows D$, where the denatured state (D) is attained from native protein through unknown intermediate states (X). In fact, an in-depth analysis of isothermal denaturation of cyt *c* by NMR spectroscopy [5,6] unambiguously identified an existence of well-defined non-native ligation geometry with His–Lys heme ligation, reminiscent of the alkaline state, at moderate concentrations of denaturants and His–His ligation of heme iron at high concentrations of denaturants in neutral pH.

The presence of stable intermediate state(s) of cyt *c* due to a perturbation of its native state (by pH and denaturants) is consistent with the so-called "foldon theory" introduced by Englander's group [11,12]. According to this theory, cyt *c* consists of five foldons (structurally independent regions) which unfold in interdependent, sequential way that constructs unfolding pathway of the protein [12]. Interestingly, in this model one of the least stable regions (foldons) is 70–85 omega loop encompassing the native ligand of heme iron, Met80, as well as the non-native ligands Lys72, Lys73 and Lys79.

In analogy with the isothermal denaturation, it is reasonable to assume a similar behavior of cyt *c* in the process of thermal denaturation. However, one of the basic works in the field of thermal stability of proteins [13] clearly showed that thermal denaturation of cyt *c* was all-or-none transition at pH ≤ 4.6, implying that cyt *c* thermal denaturation proceeds without a presence of stable intermediates. However, several more recent studies pointed out an existence of conformational transition in mitochondrial cyt *c* which occurs well before a main transition that is accompanied with a loss of its secondary structure [14–20]. Some of these works indicated that the thermal transition preceding the major transition is similar to the alkaline isomerization of cyt *c* [14,17,18,20]. However, the findings regarding an existence of the stable alkaline-like intermediate state in the thermal denaturation of cyt *c* and a nature of its final thermally-denatured state at neutral pH have not been further elaborated.

Numerous results obtained in our laboratory pointing out to a non-two-state thermal denaturation of cyt *c* at neutral and slightly acidic pH, as well as intriguing possibility of a physiological role of the alkaline-like state of cyt *c*, motivated us to perform a systematic analysis of the thermal denaturation of cyt *c* at these conditions. We have used a number of methods to investigate thermally-induced unfolding of cyt *c* over the pH range 3.5–7.5. The local stability was probed by electronic absorption and circular dichroism (CD) in the Soret region, whereas the global structural changes were studied by CD at 222 nm, intrinsic tryptophan fluorescence emission and viscosimetry. In addition, we employed differential scanning calorimetry (DSC) that has a potential to probe both local and global structural perturbations in cyt *c*. This work presents an attempt to fill up a gap in our understanding of such basic property as is the thermal stability of cyt *c* at neutral and slightly acidic pH, i.e. at its physiological pH in the intermembrane space in mitochondria.

2. Materials and methods

Horse heart cyt *c* was obtained from Sigma-Aldrich (St. Louis, MO, USA). All other chemicals were purchased from Fluka and Sigma-Aldrich. The protein was fully oxidized prior to the measurements by the addition of 1 μl of 11 mM potassium ferricyanide to 1 ml of sample. The pH of the samples was determined using a HI 9017 pH meter coupled to a HI 1330 pH electrode (Hanna Instruments Srl, Padova, Italy). All measurements were performed in 10 mM and 50 mM buffers (glycine in the pH range of 2.8–3.7, sodium acetate in the pH range of 3.6–5.5, sodium cacodylate in the pH range of 5.0–7.0, sodium phosphate in the pH range of 6.0–7.5, MOPS in the pH range of 6.5–7.5, HEPES in the pH range of 7.0–8.0, Tris–HCl in the pH range of 7.0–8.5).

2.1. Absorption measurements

Optical absorption data were collected in a Specord S 300 UV VIS and Specord S 600 diode array spectrophotometer (Analytik Jena AG, Jena, Germany) equipped with a Peltier-thermostated cell holder with a PTC 100 control unit. The temperature was changed from 25 to 95 °C with a heating rate of 1 °C/min. The protein concentration was 8 μM for measurements in the Soret region; 100 μM in the region at 500–720 nm.

2.2. Circular dichroism measurements

A Jasco J-810 spectropolarimeter (Tokyo, Japan) equipped with a Peltier type thermostatted single cell holder (PTC-423S) was used for circular dichroism measurements. Ellipticities were measured at 222 nm and 417 nm in 1 mm and 1 cm pathlength quartz cuvettes, respectively. The temperature was changed from 25 to 95 °C with a heating rate of 1 °C/min. Cyt *c* concentrations were 50 μM and 10 μM in the far-UV and the Soret regions, respectively.

2.3. Fluorescence measurements

Fluorescence measurements were performed with a Varian Cary Eclipse fluorescence spectrophotometer (Varian Australia Pty Ltd) equipped with a Peltier multicell holder. The temperature was changed from 25 to 95 °C with a heating rate of 1 °C/min. The excitation wavelength was 290 nm and emission at 350 nm was collected. The protein concentration was 8 μM.

2.4. Viscosity measurements

All viscosimetric measurements were performed on a rotational contactless viscometer VISCODENS [21]. It is a Couette-type non-contact viscometer that allows the measurement of the true bulk viscosity at a constant shear rate eliminating errors caused by the surface shear viscosity. The precision of viscosity measurements is approximately 0.1%. The volume of the sample was 1.6 ml, shear rate γ was 60/s. The solution of cyt *c* was freshly prepared before each measurement and the concentration of cyt *c* was about 242 μM (3 mg/ml). The baseline was measured for each measurement with a corresponding buffer in the absence of the protein. VISCODENS allowed the measurement of the temperature dependence in the scanning mode with the precision of ±0.02 °C. The thermal denaturation of cyt *c* at different pH values was followed with a constant scan rate of 20 °C/h. Higher scan rates were not possible due to the limitations of the viscosimeter. Reduced viscosity was calculated using an equation:

$$\eta_{red} = \frac{1}{c}\frac{\eta - \eta_0}{\eta_0} \quad (1)$$

where η_{red} is the reduced viscosity of a protein, η is the viscosity of a solution, η_0 is the viscosity of a solvent and c is a protein concentration in g/ml.

2.5. Differential scanning calorimetry measurements

DSC experiments were performed on a VP-DSC differential scanning microcalorimeter (Microcal, Northampton, MA) at a scan rate of 1 °C/min. Cyt *c* concentration was 82 μM. Measurements were carried out under a constant overpressure of 1.5 atm. A background scan, collected with a buffer in both cells, was subtracted from each sample scan. The reversibility of the transitions was assessed by the reproducibility of the calorimetric trace in a second heating cycle performed immediately after cooling from the first scan. Excess heat capacity curves were plotted using Origin software supplied by Microcal.

2.6. Analysis of the data

The individual experimental data sets (absorbance, CD or Trp fluorescence emission values) were analyzed as a single-step process (state 1 ⇄ state 2) by applying a non-linear least-squares fit based on the following equation:

$$S_{obs} = \frac{S_1 + m_1 T + (S_2 + m_2 T)\exp\left[\frac{\Delta H_{vH}}{R}\left(\frac{1}{T_{trs}} - \frac{1}{T}\right)\right]}{1 + \exp\left[\frac{\Delta H_{vH}}{R}\left(\frac{1}{T_{trs}} - \frac{1}{T}\right)\right]} \quad (2)$$

where S_1 and S_2 represent intercepts of the pre-transition and post-transition baselines with y-axis, respectively, m_1 and m_2 are the slopes of the pre-transition and post-transition baselines, respectively, ΔH_{vH} is the enthalpy change at the transition temperature T_{trs}, R is the gas constant and T is the temperature.

Analysis of thermal denaturation of cyt *c* measured by DSC at pH > 5.5 indicates that the process of its thermal denaturation has a non-two-state character and can be described by the following (minimalist) scheme:

$$N \overset{K_1}{\leftrightarrow} I \overset{K_2}{\leftrightarrow} D \quad (3)$$

where *N* is native cyt *c*, *I* is an intermediate form of cyt *c* and *D* is a thermally denatured form of the protein.

Assuming that both of the steps are reversible, the equilibrium constants are calculated by the following equations:

$$K_1 = \exp\left[\frac{\Delta H_{vH1}}{R}\left(\frac{1}{T_{trs1}} - \frac{1}{T}\right)\right] \quad (4)$$

$$K_2 = \exp\left[\frac{\Delta H_{vH2}}{R}\left(\frac{1}{T_{trs2}} - \frac{1}{T}\right)\right] \quad (5)$$

where ΔH_{vH1} is the van't Hoff enthalpy change at the transition temperature T_{trs1} and ΔH_{vH2} is the van't Hoff enthalpy change at the transition temperature T_{trs2}.

Providing that $K_1 = \frac{f_I}{f_N}$, $K_2 = \frac{f_D}{f_I}$ and $f_N + f_I + f_D = 1$, the individual fractions were calculated as follows:

$$f_N = \frac{1}{1 + K_1 + K_1 K_2} \quad (6)$$

$$f_I = \frac{K_1}{1 + K_1 + K_1 K_2} \quad (7)$$

$$f_D = \frac{K_1 K_2}{1 + K_1 + K_1 K_2}. \quad (8)$$

The fractions, f_N and f_D, dependences on temperature were used for a comparison of thermal transitions monitored by DSC with thermal transitions measured by other methods as shown in Fig. 4.

3. Results

3.1. Intrinsic probes of local conformational changes in cyt c

Absorption spectrum of cyt *c* in visible region is particularly sensitive to conformational changes in heme region (Fig. S1). The Soret band (in spectral region at 350–450 nm) sensitively reflects changes in close heme environment [22,23] and band at 695 nm is a sensitive probe of Met80-heme iron bond [24]. Moreover, band at 620 nm (absent in low-spin state of native from of cyt *c*) is an indicator of a high-spin state of heme iron in the protein, i.e. replacement of strong ligand at the 6th axial position of heme iron with a weak ligand such as water molecule [25]. Another sensitive probe of heme region is characteristic doublet in the Soret region of CD spectrum of cyt *c* (Fig. S2). The intensity of the negative band at 417 nm depends on heme–protein interactions [26] and reflects the direct interaction of $\pi \rightarrow \pi^*$ transition of the aromatic ring of Phe82 with $\pi \rightarrow \pi^*$ transition of the heme group [27]. A decrease in the intensity of the negative lobe in the Soret region sensitively reflects changes in the distance and/or orientation of the phenylalanine residue regarding the heme in cyt *c* [28]. Disappearance of 417 nm negative cotton effect, change in maximum position and amplitude of Soret band and disappearance of 695 nm in absorption spectra of cyt *c* were observed as a result of pH change, replacement of Met80–heme iron bond by extrinsic ligands (such as imidazole, cyanide, azide) [22,29], or chemical modification [15], perturbations induced by denaturants (such as urea, guanidine HCl, alcohols), by elevated temperature [22,30,31] and by complexation with model membrane surface and hydrophobic polyanions [32–34]. To monitor local conformational changes in close proximity of heme region of cyt *c*, we utilized all the discussed spectral intrinsic probes, i.e. absorbance bands in Soret region, at 620 nm and 695 nm as well as CD signal at 417 nm.

The CD spectrum of cyt *c* in the near-UV region provides information regarding environment around aromatic aminoacid residues (Fig. S2). The spectrum is characterized by: (i) two sharp minima at 282 nm and 288 nm assigned to the Trp59 side chain [22,35], and (ii) two overlapping bands centered around 251 nm and 262 nm attributed to tyrosine side chains and porphyrin transitions, respectively [22,36]. However, these bands are relatively insensitive to local heme perturbations induced by extrinsic ligands or pH variations [22].

3.2. Monitoring of global conformational changes

To monitor global thermally-induced changes in cyt *c* we used: (i) the band 222 nm in the far-UV CD spectrum, (ii) fluorescence of Trp59, (iii) viscosimetry, and (iv) method of differential scanning calorimetry (DSC).

The 222 nm band in the CD spectrum is a well-known sensitive probe for α-helical secondary structure of proteins. In fact, the structural unit (or foldon) formed by amino- and carboxyl-terminal helices is the most stable structure in cyt *c*, unfolding of which indicates global destabilization of the protein [11,12].

Cyt *c* contains suitably located internal fluorescence probe — single tryptophan, Trp59, which is in a native state quenched by close heme due to resonance energy transfer [37–39] (Fig. 1). The sharp distance dependence of the fluorescence quenching and fluorescence zero baseline amplitude make it exceedingly sensitive to structural changes occurring around the heme [37,38,40–42]. Structural perturbation of deeply buried Trp59 accompanied by appearance of its fluorescence is another indication of global destabilization of cyt *c*.

Viscosimetry represents a suitable method for the study of spatial protein distribution. Based on the experimental results using viscosimetry either on its own or in combination with other methods mentioned above that allow the monitoring of the global conformational changes we can deeply describe the conformational changes of the protein at the level of tertiary structure.

DSC is an experimental method that enables us to monitor thermally-induced conformational changes of proteins by measuring amounts of absorbed (or released) heat which accompanies such changes [43,44].

3.3. Thermally-induced transitions of cyt c in neutral and acidic pH values

Fig. 2A shows transition temperatures of thermally-induced transitions in dependence on pH obtained from measurements monitored by absorbance and CD spectroscopy intrinsic probes, tryptophan fluorescence, viscosimetry, and DSC. This dependence may be formally divided into two parts: (i) pH ≤ 5.0 and (ii) pH ≥ 5.0. The breaking point, at pH ~5.0, corresponds to an appearance of high-spin state of heme iron in a thermally-denatured state (95 °C) as indicated by sigmoidal dependence of the band at 620 nm with $pK_a = 4.9 \pm 0.2$ at given conditions (Fig. 2A). In the pH range below pH 5.0 transition temperatures obtained by all utilized methods, i.e. methods monitoring both local and global conformational changes, are overlapping. At pH ~5.0, however, the dependence splits into two branches in the pH range of 5.0–7.5 (Fig. 2). The "upper" branch represents transition temperatures that slightly increase with pH while in the "lower" branch the transition temperatures decrease markedly with pH. Noteworthily, the upper branch of the dependence consists of transition temperatures obtained by the probes/methods detecting global structural changes in cyt *c* such as CD at 222 nm, tryptophan fluorescence and DSC (major transition observed at higher temperatures, see below). On the other hand, the lower branch consists of transition temperatures obtained by monitoring local conformational changes such as absorbance and CD of Soret band, and absorption band at 695 nm and CD signal at 417 m. The transition temperature of the first (of two) thermal event monitored by DSC falls into the lower branch dependence of the transition temperatures.

Analogous dependence is evident from a plot of van't Hoff enthalpies of the thermal transitions vs the pH value of solvent (Fig. 2B). The shown dependences indicate the local thermally-induced conformational changes, which occur at lower transition temperatures, and are accompanied with lower van't Hoff enthalpies than the global thermally-induced conformational changes.

In general, an apparent enthalpy value is significantly affected by the presence of intermediate(s) and/or irreversible step(s) in denaturation process. In the former case, the presence of intermediate(s) causes a decrease in an apparent value of derived van't Hoff enthalpy. In the latter one, an irreversible step in protein denaturation leads to sharper and asymmetrical transition which results in an increase of an apparent value of van't Hoff enthalpy. The presence of intermediate(s) affects an apparent enthalpy of denaturation only when the intermediate(s) are hidden, i.e. two or more transitions are not properly distinguished from each other. In the present work, this is the case of thermal transitions of cyt *c* in the pH region close to the branching point at pH ~5. In fact, values of the apparent van't Hoff enthalpies of cyt *c* transitions are the most spread in the pH range of 5.0–5.5 (Fig. 2B). Thermal transitions at pH < 5 have a two-state character, while on the other hand, at pH > 5.5 the thermal transitions are relatively well separated. Reversibility of thermal transition of cyt *c* decreases with increasing value of pH from more than 90% at pH ~5 to 60–70% at pH ~7.5. Moreover, reversibility of thermal transitions steeply decreases with protein concentration. Although thermal transition of cyt *c* corresponding to global unfolding is quite symmetrical (measured by DSC as well as optical methods) (Fig. 3) an irreversible step apparently affects van't Hoff enthalpy of the transition. In fact, the dependence of irreversible step on protein concentration suggests an explanation why the van't Hoff enthalpies derived from DSC experiments (at cyt *c* concentration 80 μM) are significantly higher than the ones derived from experiments performed at nearly 10-fold lower concentration by optical methods at neutral pH. Therefore, obtained van't Hoff enthalpies do not allow us to unambiguously interpret their values in regard to cooperativity of thermal transitions of cyt *c* in the pH range of 5.0–7.5. However, on the other hand, different values of van't Hoff enthalpies obtained by diverse experimental techniques at pH < 5.0, i.e. when thermal transitions of cyt *c* have a two-state character, suggesting that cooperativity of cyt *c*

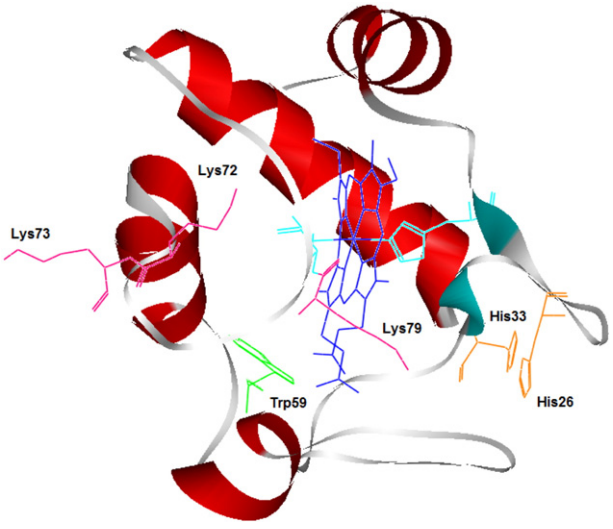

Fig. 1. Structure of native horse heart cyt *c* (1HRC.pdb [39]). Potential non-native axial ligands (His26, His33, Lys72, Lys73, and Lys79) as well as Trp59 are depicted by their side chains.
Visualized by WebLab ViewerLite version 4.0 software (Accelrys, San Diego, California).

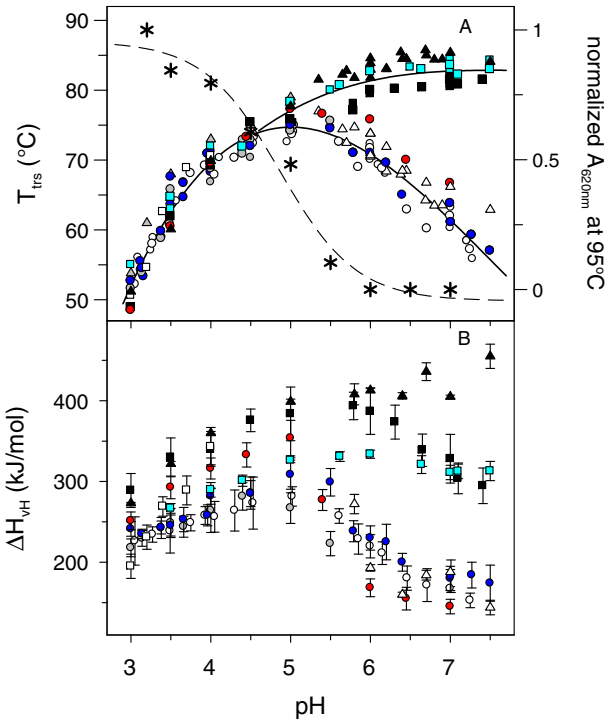

Fig. 2. Dependence of cyt *c* transition temperatures (A) and van't Hoff enthalpies (B) of the thermal transitions on pH monitored by absorbance at 396 nm (white circles), 620 nm (gray circles) and 695 nm (blue circles), Trp fluorescence (black squares), CD at 222 nm (cyan squares), and 417 nm (red circles), viscosity (white squares) and DSC (black and white triangles). Data obtained by methods detecting local and global conformational changes are shown by circles and squares, respectively. Data obtained by DSC are shown by triangles. The solid lines serve as a lead for eyes for dependences of transition temperatures on pH. Asterisks represent normalized values of absorbance at 620 nm in thermally-denatured state (at 95 °C) of cyt *c*. The dashed curve represents fit of a pH-dependence of the normalized values at 620 nm with $pK_a = 4.9 \pm 0.2$.

thermal transition is different in different parts of cyt *c* in consistency with the foldon theory [11,12].

Data shown in Fig. 2 are obtained from sigmoidal dependencies of signals monitored by UV–VIS and CD spectroscopies, tryptophan fluorescence and DSC such as shown in Fig. 3. The normalized dependencies of thermal transitions at pH 4, 5, 6, and 7 (Fig. 3) show that a difference between transition temperatures of local changes in the heme region and the global changes diminishes with decreasing pH.

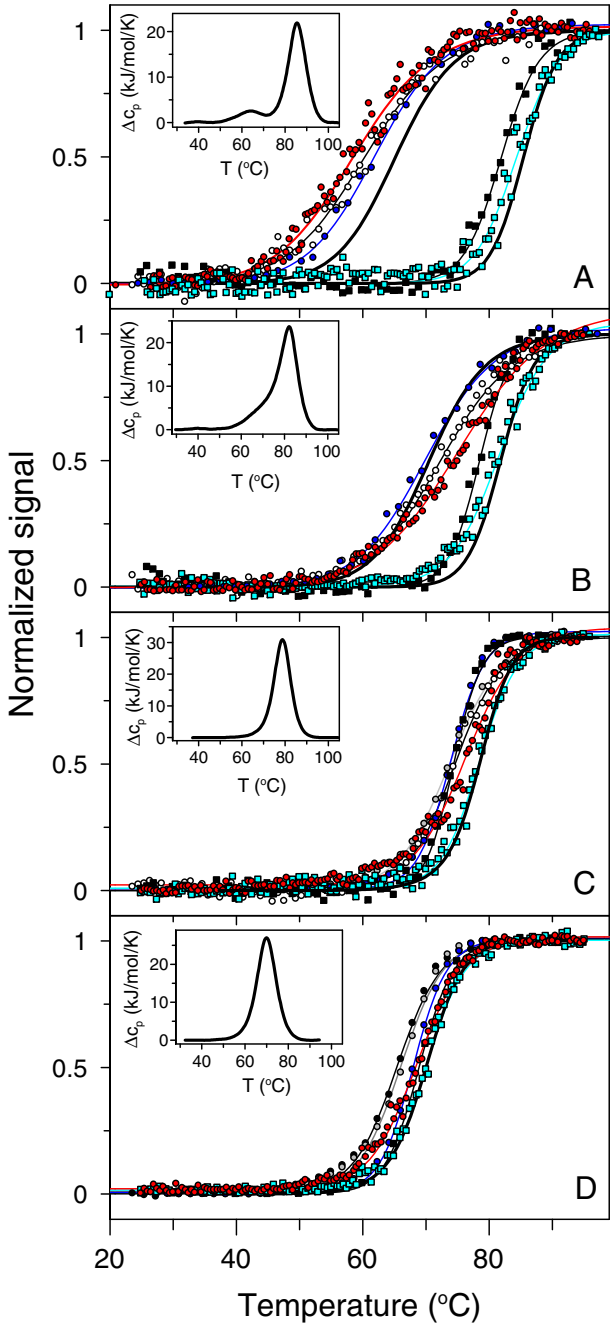

Fig. 3. Normalized thermal denaturation dependences of cyt *c* obtained at different pH values: pH 7.0 (A), pH 6.0 (B), pH 5.0 (C) and pH 4.0 (D). Thermal denaturations were monitored by absorbance at 396 nm (white circles), 620 nm (gray circles) and 695 nm (blue circles), Trp fluorescence (black squares), CD at 222 nm (cyan squares), and 417 nm (red circles), and DSC (thick solid lines). Sigmoidal curves are non-linear least square fits to Eq. (2). Insets: DSC thermogram (corrected on baseline) of cyt *c* at corresponding pH.

DSC is a sensitive technique able to sense both thermally-induced conformation transitions in cyt *c* that are detected separately either by the local or by global intrinsic spectral probes (insets in Fig. 3).

3.4. Thermally-induced transitions of cyt c in neutral and acidic pH values measured by DSC

DSC measurements of cyt *c* show an intricate dependence on pH (insets in Figs. 3, S3) in analogy with transition temperature dependence on pH shown in Fig. 2. Below pH ~5 thermal transitions of cyt *c* are of all-or-none nature as follows from the fact that the ratio of van't Hoff and calorimetric enthalpies (obtained from the same DSC experiment) is close to value one (Table S4), i.e. thermal transitions of cyt *c* at pH ≤5 comply with the necessary condition for all-or-none thermal transition [13]. The transitions are highly reversible (>95%) what was assessed from re-scanning of re-cooled thermally-denatured protein. At pH ≥5, the thermal transitions of cyt *c* are more complex as indicated by the presence of two apparent transitions in DSC profile (insets in Figs. 3, S3). Although reversibility of the transitions decreases with increasing pH, it is still reasonably high (~60–70%) at the neutral pH. It needs to be stressed that both DSC profile of cyt *c* and the reversibility of its thermal transitions are fairly independent on the used buffer (MOPS, HEPES, phosphate buffer, sodium cacodylate) as well as on the buffer concentration within studied concentration range (10–50 mM) at the neutral pH. The exception is the buffer Tris–HCl (Fig. S4) due to its strong pH dependence on temperature, $d\mathrm{pH}/d\mathrm{T}$ ~−0.028 pH units/deg [45]. In fact, a pH value of Tris–HCl solution with pH 7.4 prepared at 20 °C decreases to pH ~6.0 at 70 °C. This is well indicated by a shift of the lower branch of cyt *c* transition temperatures measured in 50 mM Tris–HCl buffer by more than ~1 pH unit to higher pH values (Fig. S5) as well as from the observation that DSC profile of cyt *c* measured in Tris–HCl at pH 8.0 is comparable to DSC profile of cyt *c* measured in other buffers (of which pH is temperature independent) at pH ~7.0 (Fig. S4).

3.5. Non-two-state thermal denaturation of cyt c

Based on the above results, thermal transition of cyt *c* consists of two apparent steps and can be described by the minimalist scheme (3): $N \leftrightarrow^{T_{local}} I \leftrightarrow^{T_{global}} D$, where *N*, *I* and *D* are native, intermediate and thermally-denatured (final) states of cyt *c*, respectively. Calculation of temperature dependence of fractional populations of individual states of cyt *c* at different pH values according to Eqs. (6)–(8) based on parameters obtained from the thermal transitions of cyt *c* presented in Fig. 3 is summarized in Fig. 4. Obtained fractional populations of native, intermediate, and final thermally-denatured states of cyt *c* show their dependence on pH. The population of the intermediate state(s) is maximal at pH 7.0 when it reaches the fractional population 85–90% at ~70–75 °C (Fig. 4, upper part). The population of the intermediate state(s) significantly decreases with decreasing pH and becomes negligible at pH ≤5.0 (Fig. 4, middle and lower parts).

3.6. Properties of the intermediate and the final thermally-denatured states of cyt c monitored by local and global conformational probes

The methods sensitive to local conformational changes, such as absorbance and CD differential spectra in the Soret region, enabled us to closely analyze: (i) the intermediate state of cyt *c* at pH 7.0 and (ii) pH dependence of the final thermally-denatured states of cyt *c*. The differential spectra of the intermediate and the final thermally-denatured states were obtained by subtracting of cyt *c* spectrum at 25 °C from the spectrum obtained at 75 °C and 95 °C, respectively (Fig. 5). For comparison purposes, the differential spectra obtained by subtracting native spectrum (obtained at pH 7.0) from alkaline (obtained at pH 11.0) at 25 °C are also presented for absorbance (inset Fig. 5A) and CD (Fig. 5B).

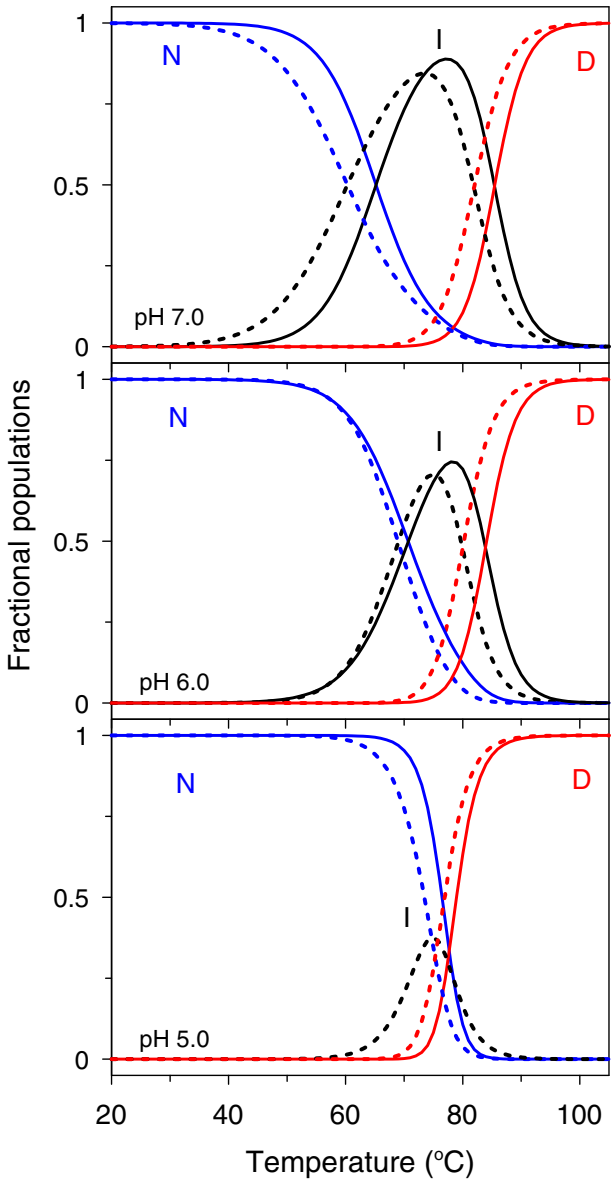

Fig. 4. Fractions of the three predominant states populated in the thermally-induced transitions of cyt *c* at pH 7.0, 6.0 and 5.0. The fractions were calculated using Eqs. (6)–(8). Solid lines represent fractions calculated from DSC results (parameters T_{trs1}, T_{trs2}, ΔH_{vH1}, ΔH_{vH2} listed in Table S4) whereas dashed lines are those obtained from absorbance measurements at 396 nm (T_{trs1}, ΔH_{vH1} listed in Table S1) and Trp fluorescence results (T_{trs2}, ΔH_{vH2} listed in Table S3).

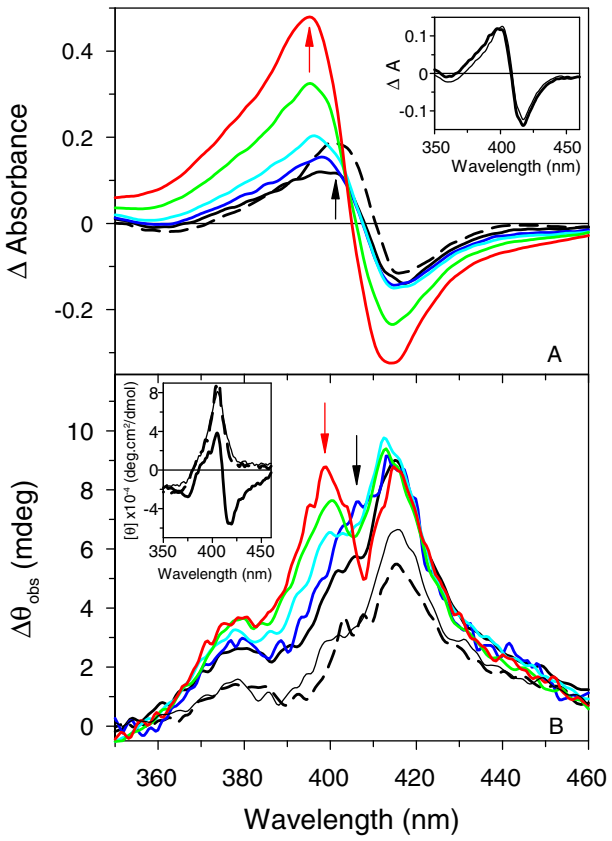

Fig. 5. Differential absorbance (A) and CD (B) spectra of cyt *c* in the Soret region obtained by subtracting spectrum of cyt *c* at 25 °C from spectra at 95 °C at different pH values: pH 7.0 (black solid line), pH 6.0 (blue solid line), pH 5.0 (cyan solid line), pH 4.0 (green solid line), and pH 3.5 (red solid line). For comparison purposes a differential spectrum of the alkaline state of cyt *c* at 25 °C (black dashed line) is shown . Inset in box A: Comparison of absorbance differential spectra of cyt *c* 75–25 °C (thin line) and 95–25 °C (thick line). Arrows in box A indicate position of maxima in the differential spectra for the alkaline state (black) and for the final thermally-denatured state of cyt *c* at pH 3.5 (red). Inset in the box B: CD spectra of cyt *c* in the native state at 25 °C, pH 7.0 (thick solid line) and in its alkaline state pH 10.5 (thick dashed line), and in the thermally-denatured state at 75 °C, at pH 7.0 (thin solid line), in the Soret region expressed in molar ellipticity. In box B, black arrow indicates position of a shoulder in the differential spectra for the alkaline state and for the final thermally-denatured state of cyt *c* at pH 7.0 and red arrow designates newly formed maximum in the differential spectrum of the thermally-denatured state at decreased pH. Concentrations of cyt *c* were 8 μM and 10 μM for absorbance and CD measurements, respectively.

The absorbance differential spectrum of intermediate state of cyt *c* at pH 7.0 indicates a resemblance of the thermally-denatured state with the alkaline state of cyt *c*. This follows from the fact that the maxima and minima of both differential spectra are at the same wavelengths, ~402 nm and ~416 nm, respectively, and amplitudes of both differential spectra are similar (inset Fig. 5A). The absorbance differential spectrum of the final thermally-denatured state at pH 7.0 is also similar to the alkaline state of cyt *c*, but with decreasing pH its maximum shifts towards ~394 nm pointing out to a formation of different conformational state(s).

Analogously, the differential CD spectrum of the intermediate state of cyt *c*, obtained by subtracting the spectrum recorded at 25 °C from the one recorded at 75 °C at pH 7.0, is similar in shape and amplitude with the differential spectrum of cyt *c* in the alkaline state, i.e. maximum positioned at ~417 nm and a shoulder at ~404 nm. The differential CD spectrum of the final thermally-denatured and the alkaline states of cyt *c* are comparable in the shape but the amplitude of the thermally-denatured state is higher. Decreasing pH does not affect the position and the amplitude of the thermally-denatured state of cyt *c* but leads to an appearance of another maximum at ~400 nm indicating formation of another conformational state(s).

The methods monitoring global conformational changes in cyt *c* such as intrinsic tryptophan fluorescence and reduced viscosity are insensitive towards conformational changes of cyt *c* in the intermediate and alkaline states. This conclusion follows from the absence of changes in tryptophan fluorescence and reduced viscosity of cyt *c* both at 75 °C in pH 7.0 and at the alkaline state of cyt *c* (Figs. 6, 7) [46,47]. On the other hand, the appearance of tryptophan fluorescence in the final thermally-denatured cyt *c* at pH 7.0 points out a global conformational change of the protein. Although reduced viscosity of cyt *c* was not possible to determine for temperatures over 80 °C, obtained data indicate a slight increase in the reduced viscosity at ≥75 °C supporting thus a global conformational change observed by the fluorescence. Decreasing pH leads to significant destabilization of cyt *c* following from a decreasing transition temperature observed by Trp59 fluorescence (Fig. 6). Unfortunately, strong quenching of tryptophan fluorescence with increasing

temperatures hampered a comparison of the thermally-denatured states of cyt *c* at different pH values. On the other hand, reduced viscosity value of the thermally-denatured cyt *c* at pH ~4.0 strongly indicates that cyt *c* is in a highly compact state even at such destabilizing conditions. In fact, even at pH 3.5 when cyt *c* is strongly destabilized as indicated by the low transition temperature obtained from tryptophan fluorescence measurements (Fig. 6), its reduced viscosity is still by ~40–50% lower the value of cyt *c* in fully extended denatured state (~22 ml/g) [40].

4. Discussion

The results of the present study: (i) show, for the first time, non-two-state nature of thermal denaturation of cyt *c* at neutral *and slightly acidic pH*, (ii) in accordance with previous findings, indicate a similarity of the intermediate state in thermal denaturation with the alkaline-like state of cyt *c*, and (iii) for the first time suggest, in analogy with isothermal denaturation studies, bis-histidinyl ligation of the heme iron in the final thermally-denatured state of cyt *c* in the pH range of ~5.0–7.5.

4.1. Non-two-state thermal denaturation of cyt c at neutral pH

Although the authors of several previous studies noticed sequential events in the thermal denaturation of cyt *c* in neutral pH [14,16–20,49], the novelty of our work is that we show that the intermediate state is present not only at neutral pH but also at acidic pH, i.e. in the pH range from ~5 to pH 7.5. The population of the intermediate state significantly decreases with decreasing pH and at pH ~5 is negligible.

4.2. Resemblance of the intermediate state of cyt c thermal denaturation at neutral and slightly acidic pH values with its alkaline state

The intermediate state of cyt *c* formed in thermal denaturation is characterized by native-like global conformation with a local conformational change in its heme region. The native-like, i.e. highly compact, global conformation can be deduced from (i) the absence of changes in the protein secondary structure monitored by ellipticity in the far-UV CD, (ii) the intact tertiary structure as indicated by an absence of Trp59 fluorescence and identical reduced viscosity as the native state, (iii) the maintenance of the low-spin state of heme iron as indicated by an absence of the 620 nm band in absorbance spectroscopy, and (iv) an observation that a formation of the intermediate state is accompanied by only small calorimetric enthalpy. However, the intermediate state differs from the native state of cyt *c* by local conformational change in the heme region reflected by: (i) disappearance of the band 695 nm, (ii) decrease in amplitude of negative cotton effect at 417 nm and (iii) change in the Soret absorption band. Interestingly, native-like nature of cyt *c* as well as observed spectral properties of the intermediate state in thermal denaturation of cyt *c* at neutral and slightly acidic pH values are similar to properties of its alkaline state formed in alkaline pH with pK_a ~ 9.0–9.3 at low ionic strength [50]. In fact, the same conclusion regarding a resemblance of thermally-denatured state of cyt *c* with its alkaline state has been reached by authors of several previous studies [14,17,18,20]. Interestingly, this is in accordance with conclusions drawn from isothermal denaturation studies of cyt *c* by denaturants such as GdnHCl and urea at neutral pH pointing out on an existence of alkaline-like intermediate state in the unfolding process [5,6]. This leads to an intriguing conclusion that cyt *c* unfolding proceeds through common intermediate states independent on a triggering factor (chemical denaturant or temperature) of the unfolding process. Although lysine is quite an unexpected ligand for heme iron at neutral pH (due to a high value of pK_a ~ 11 of amine group in a lysine side chain), high effective concentration of lysine residues (Lys72, Lys73 and Lys79) around the 6th ligand position of the heme iron and strong Lys–heme iron bond causes the formation of the alkaline-like state at neutral pH after Met80–heme iron bond perturbation. In fact, destabilization of heme pocket, more specifically the 70–85 omega loop foldon by: (i) mutation, e.g. Phe82 [51], (ii) Hofmeister anions [52], (iii) modification of dielectric constant of solvent, e.g. in the presence 30% acetonitrile in water [53], (iv) chemical denaturant [5,6], or (v) increased temperature [14,17,18,20, the present work] may drive displacement of Met by Lys even near neutral pH.

Noteworthy, the present work also shows that the transition $N \leftrightarrow^{T_{local}} I$ can be detected by DSC. The presence of two distinct steps in the thermal denaturation of cyt *c* monitored by DSC was noticed in two previous studies [15,32] where the low-temperature event was interpreted as loosening of protein structure in the vicinity of heme crevice. We show that the low-temperature event is highly reproducible but strongly pH-dependent as it is demonstrated by measurements performed in Tris–HCl buffer (Fig. S5). The transition temperature of this step obtained from DSC is in excellent consent with those obtained from local (spectral) probes strongly indicating that this transition represents a conformational change in the heme region of cyt *c* due to replacement of Met80 for another strong-field ligand(s), lysine(s).

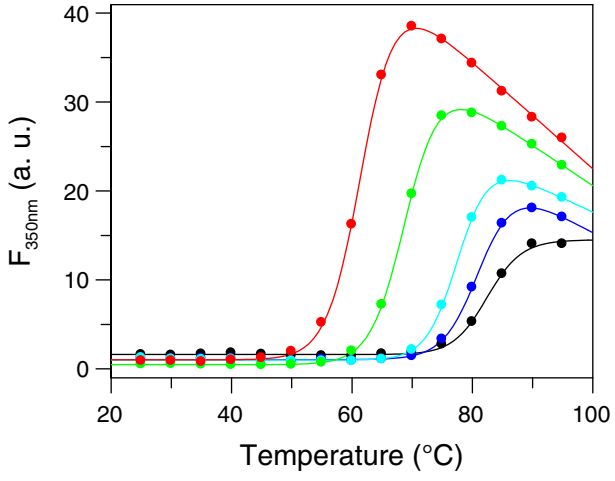

Fig. 6. Thermal denaturation of cyt *c* monitored by tryptophan fluorescence at different pH values: pH 7.0 (black circles), pH 6.0 (blue), pH 5.0 (cyan), pH 4.0 (green), and pH 3.5 (red).

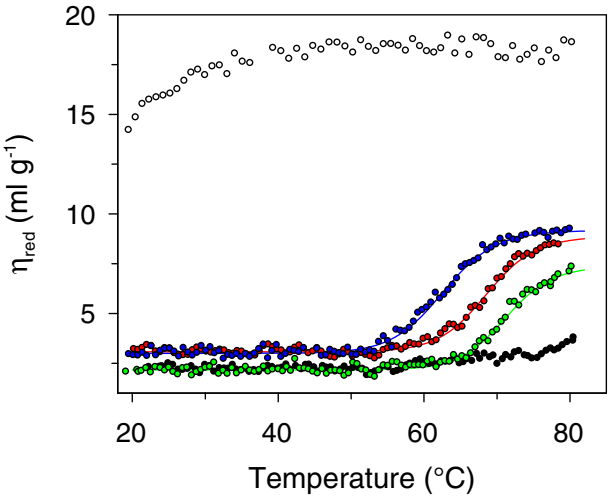

Fig. 7. Thermal denaturation of cyt *c* monitored by reduced viscosity at different pH values: pH 7.0 (black circles), pH 4.0 (green), pH 3.7 (red), pH 3.4 (blue), and pH 2.0 (white). Reduced viscosity of native state of cyt *c* is ~2.9 ml/g [48]. For comparison, thermal dependence of reduced viscosity of cyt *c* at pH 2.0, i.e. at conditions when cyt *c* is in highly extended state, is shown.

4.3. The final thermally-denatured states differ in pH ≤5 and in the pH range from ~5 to 7.5

The high-temperature event, $I \leftrightarrow^{T_{global}} D$, i.e. formation of the final thermally-denatured state, accompanied with global structural changes such as significant decrease in secondary structure indicated by a decrease in amplitude of CD signal at 222 nm and perturbation of the hydrophobic core of cyt *c* demonstrated by an appearance of Trp59 fluorescence and an increase in reduced viscosity is even less understood than the formation of the intermediate state. The final thermally-denatured state cannot be considered as unstructured state with expanded structure as the heme iron is in the low-spin state indicating the presence of a strong-field ligand at the 6th ligand position. The existence of the low-spin heme iron along with a significant structural perturbation of cyt *c* in the final thermally-denatured state strongly indicates that cyt *c* forms where the strong-field ligand in intermediate state (Lys72/Lys73/Lys79) is replaced by another strong-field ligand, very likely one of histidines 26/33. This conclusion follows from: (i) assumption of analogous conformational states in isothermal and thermal denaturation of cyt *c* [6,54], and (ii) similarity of His pK_a value with the pH value of ~5.0 at which two branches of transition temperatures merge (Fig. 2), and (iii) the observation that the nature of the finally-denatured state changes from low (pH > 5) to high spin (pH ≤ 5) state of heme iron. If histidine occupies the 6th position of the heme iron in the final thermally-denatured state at pH ≤ 5, its side chain becomes protonated and unable to serve as the ligand for heme iron and leaves the 6th ligand position available for a weak-field ligand most likely a water molecule. In fact, the existence of pH-induced conformational transition of denatured form of cyt *c* (from a compact form at neutral pH to an extended form at acidic pH) with pK_a ~5.0–5.1 strongly indicates an analogy with our results [31,37,40]. Involvement of His26 but preferably His33 as the 6th ligand of heme iron during chemically-induced unfolding or refolding from chemically-denatured state is well documented [49,54–57]. Interpretation of the results presented in this work in accordance with previous analysis is summarized in Fig. 8.

4.4. Effect of pH on thermal denaturation of cyt c at different pH values and possible physiological implications

Cyt *c* has been shown to perform many physiological functions in the mammalian cell [58]. Besides its well-known function as a shuttle of electrons between cyt bc_1 and cyt *c* oxidase, it has both antioxidant and peroxidase-like activities and after release from mitochondria it participates at initiation stages of apoptosis [9,59–62]. All of these functions depend on a particular conformation state, stability of which depends on pH and properties of its close environment. Thus two populations of cyt *c* located in intermembrane mitochondrial space, i.e. membrane-bound and free fractions, might face to different regulation by the surrounding pH value. While the relative size of membrane-bound fraction of cyt *c* can be modulated by ATP/ADP ratio and/or protein phosphorylation [58], pH value of intermembrane space can be effective modulator both the fraction of protein bound to membrane as well as conformational state of cyt *c* with functional consequences. Decreased pH in intermembrane space in mitochondria, as well as local decrease of dielectric constant near the membrane surface, might significantly affect stability both native (free) and alternative states of cyt *c* in membrane-bound form [63,64]. In fact, experiments mimicking such environment indicate formation of alkaline-like conformation of cyt *c* [53,65]. However, cyt *c* in alkaline state loses its ability to shuttle electrons between complexes in the respiratory chain as well as its peroxidase activity [66]. Reversible formation of alkaline-like (His18/LysX) intermediate might thus serve for cyt *c* as an efficient defensive mechanism against reactive oxygen species. On the other hand, an increase of transition temperature with decreasing pH (in the pH range of 5–7.5) works in opposite direction as it increases stability of functional (His18/Met80) form of cyt *c* over its alkaline-like state.

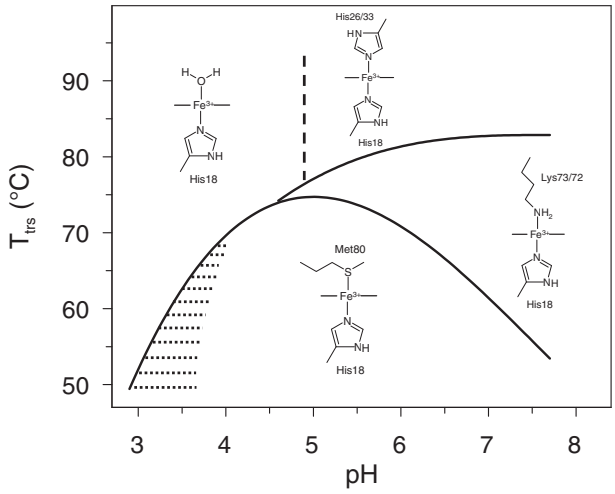

Fig. 8. Schematic phase diagram of thermally-induced transitions of cyt *c* in dependence of pH. The structures indicate heme iron ligands at given conditions. The solid lines are obtained from dependences of transition temperatures on pH shown in Fig. 2A. The dashed line approximately divides pH regions at which the final thermally-denatured state of cyt *c* is predominantly in high-spin (pH ≤ 5.0) and in low-spin (pH ≥ 5.0) states of heme iron. The dotted area indicates approximate pH region at which cyt *c* forms acidic state.

Acidification of intermembrane space due to electron-transfer accompanied proton-pumping activity of complexes in the inner mitochondrial membrane might thus be important to secure sufficient fraction of functional cyt *c*. Further decrease in pH, below pH ~5, leads to an increase of net positive charge of cyt *c* with increased affinity towards negatively charged membrane surface. In an extreme situation, in onset of apoptosis, the interaction cyt *c*-membrane surface strengthened by enrichment of negatively charged phospholipid cardiolipin outer leaflet of inner membrane significantly decreases redox potential of heme iron and turns cyt *c* into a peroxidase [67–69]. In such case, cyt *c* should be in an extended, bis-histidinyl or high-spin state conformation. Indeed, very recently it has been found that cyt *c* in complex with cardiolipin is in His18/HisX conformation [70]. Noteworthily, the presence of lysines in corresponding positions of Lys72, Lys73 and Lys79 in horse heart cyt *c* in all (113 species [71]) mitochondrial cyt *c*, as well as in corresponding positions of potential non-native histidine ligands in all but one [6], indirectly indicates an important role of these residues for proper conformation and/or function of cyt *c* in their physiological environment.

5. Conclusion

Thermally-induced denaturation of cyt *c* proceeds in two different ways in dependence on pH of solution. In neutral and slightly acidic pH, the protein unfolds in two distinct steps. In the first step, the native sixth axial ligand, Met80, is replaced with a non-native lysine residue(s) from the omega loop that is subsequently, at increased temperature, replaced by a non-native histidine residue. On the other hand, in pH close to 5.0 and below prevails a simple model of the two-state unfolding from low-spin native state to high-spin state when native axial ligand is replaced by weak-field ligand, e.g. water molecule. DSC is the only technique able to monitor both consecutive steps that proceed in the pH range of 5.0–7.5 in a single experiment. Such multiple, pH-sensitive reversible conformational switches (Met80 ↔ Lys, Lys ↔ His, His ↔ H_2O) might be of physiological importance for cyt *c* function in the mitochondrial intermembrane space.

Acknowledgments

This work was supported by research grants from the Slovak Grant Agency VEGA (project nos. 1/0521/12 and 2/0062/14) and from CELIM (316310) funded by 7FP EU (REGPOT). We are grateful to Slovak

Research and Development Agency for a financial support through a project APVV-0280-11. We also thank Ivana Petrenčáková for her editorial help in preparing the manuscript.

Appendix A. Supplementary data

Supplementary data to this article can be found online at http://dx.doi.org/10.1016/j.bpc.2015.05.002.

References

[1] J. Babul, E. Stellwagen, The existence of heme-protein coordinate-covalent bonds in denaturing solvents, Biopolymers 10 (1971) 2359–2361.
[2] H. Theorell, Å. Åkesson, Studies on cytochrome c. II. The optical properties of pure cytochrome c and some of its derivatives, J. Am. Chem. Soc. 63 (1941) 1812–1818.
[3] X. Hong, D.W. Dixon, NMR study of the alkaline isomerization of ferricytochrome c, FEBS Lett. 246 (1989) 105–108.
[4] J.C. Ferrer, J.G. Guillemette, R. Bogumil, S.C. Inglis, M. Smith, A.G. Mauk, Identification of Lys79 as an iron ligand in one form of alkaline yeast iso-1-ferricytochrome c, J. Am. Chem. Soc. 115 (1993) 7507–7508.
[5] B.S. Russell, R. Melenkivitz, K.L. Bren, NMR investigation of ferricytochrome c unfolding: detection of an equilibrium unfolding intermediate and residual structure in the denatured state, Proc. Natl. Acad. Sci. U. S. A. 97 (2000) 8312–8317.
[6] B.S. Russell, K.L. Bren, Denaturant dependence of equilibrium unfolding intermediates and denatured state structure of horse ferricytochrome c, J. Biol. Inorg. Chem. 7 (2002) 909–916.
[7] M. Assfalg, I. Bertini, A. Dolfi, P. Turano, A.G. Mauk, F.I. Rosell, H.B. Gray, Structural model for an alkaline form of ferricytochrome c, J. Am. Chem. Soc. 125 (2003) 2913–2922.
[8] F. Sinibaldi, B.D. Howes, E. Droghetti, F. Polticelli, M.C. Piro, D. Di Piero, L. Fiorucci, M. Coletta, G. Smulevich, R. Santucci, Role of lysines in cytochrome c-cardiolipin interaction, Biochemistry 52 (2013) 4578–4588.
[9] N.A. Belikova, Y.A. Vladimirov, A.N. Osipov, A.A. Kapralov, V.A. Tyurin, M.V. Potapovich, L.V. Basova, J. Peterson, I.V. Kurnikov, V.E. Kagan, Peroxidase activity and structural transitions of cytochrome c bound to cardiolipin-containing membranes, Biochemistry 45 (2006) 4998–5009.
[10] Y.P. Myer, L.H. MacDonald, B.C. Verma, A. Pande, Urea denaturation of horse heart ferricytochrome c. Equilibrium studies and characterization of intermediate forms, Biochemistry 19 (1980) 199–207.
[11] Y. Bai, T.R. Sosnick, L. Mayne, S.W. Englander, Protein folding intermediates: native-state hydrogen exchange, Science 269 (1995) 192–197.
[12] M.M.G. Krishna, Y. Lin, J.N. Rumbley, S.W. Englander, Cooperative omega loops in cytochrome c: role in folding and function, J. Mol. Biol. 331 (2003) 29–36.
[13] P.L. Privalov, N.N. Khechinashvili, A thermodynamic approach to the problem of stabilization of globular protein structure: a calorimetric study, J. Mol. Biol. 86 (1974) 665–684.
[14] J. Ångström, G.R. Moore, R.J.P. Williams, The magnetic susceptibility of ferricytochrome c, Biochim. Biophys. Acta 703 (1982) 87–94.
[15] R. Santucci, A. Giartosio, F. Ascoli, Structural transitions of carboxymethylated cytochrome c: calorimetric and circular dichroic studies, Arch. Biochem. Biophys. 275 (1989) 496–504.
[16] A. Filosa, A.M. English, Probing local thermal stabilities of bovine, horse, and tuna ferricytochromes c at pH 7, J. Biol. Inorg. Chem. 5 (2000) 448–454.
[17] G. Taler, A. Schejter, G. Navon, I. Vig, E. Margoliash, The nature of the thermal equilibrium affecting the iron coordination of ferric cytochrome c, Biochemistry 34 (1995) 14209–14212.
[18] A. Filosa, A.A. Ismail, A.M. English, FTIR-monitored thermal titration reveals different mechanisms for the alkaline isomerization of tuna compared to horse and bovine cytochromes c, J. Biol. Inorg. Chem. 4 (1999) 717–726.
[19] A. Filosa, Y. Wang, A.A. Ismail, A.M. English, Two-dimensional infrared correlation spectroscopy as a probe of sequential events in the thermal unfolding of cytochromes c, Biochemistry 40 (2001) 8256–8263.
[20] L. Banci, I. Bertini, G.A. Spyroulias, P. Turano, The conformational flexibility of oxidized cytochrome c studied through its interaction with NH_3 and at high temperatures, Eur. J. Inorg. Chem. (1998) 583–591.
[21] M. Bánó, I. Strhársky, I. Hrmo, A viscosity and density meter with a magnetically suspended rotor, Rev. Sci. Instrum. 74 (2003) 4788–4793.
[22] Y.P. Myer, Conformation of cytochromes. III. Effect of urea, temperature, extrinsic ligands, and pH variation on the conformation of horse heart ferricytochrome c, Biochemistry 7 (1968) 765–776.
[23] Y.P. Myer, S. Kumar, K. Kinnally, J. Pande, Methionine-oxidized horse heart cytochromes c. II. Conformation and heme configuration, J. Protein Chem. 6 (1987) 321–342.
[24] A. Schejter, P. George, The 695-mμ band of ferricytochrome c and its relationship to protein conformation, Biochemistry 3 (1964) 1045–1049.
[25] L.S. Kaminsky, M.J. Byrne, A.J. Davison, Iron ligands in different forms of ferricytochrome c: the 620-nm band as a probe, Arch. Biochem. Biophys. 150 (1972) 355–361.
[26] Y.P. Myer, Conformation of cytochromes. II. Comparative study of circular dichroism spectra, optical rotatory dispersion, and absorption spectra of horse heart cytochrome c, J. Biol. Chem. 243 (1968) 2115–2122.
[27] S.P. Rafferty, L.L. Pearce, P.D. Barker, J.G. Guillemette, C.M. Kay, M. Smith, A.G. Mauk, Electrochemical, kinetic, and circular dichroic consequences of mutations at position 82 of yeast iso-1-cytochrome c, Biochemistry 29 (1990) 9365–9369.
[28] J. Zheng, S. Ye, T. Lu, T.M. Cotton, G. Chumanov, Circular dichroism and resonance Raman comparative studies of wild type cytochrome c and F82H mutant, Biopolymers 57 (2000) 77–84.
[29] L.A. Davis, A. Schejter, G.P. Hess, Alkaline isomerization of oxidized cytochrome c. Equilibrium and kinetic measurements, J. Biol. Chem. 249 (1974) 2624–2632.
[30] L.S. Kaminsky, F.C. Yong, T.E. King, Circular dichroism studies of the perturbations of cytochrome c by alcohols, J. Biol. Chem. 247 (1972) 1354–1359.
[31] M. Fedurco, J. Augustynski, C. Indiani, G. Smulevich, M. Antalík, M. Bánó, E. Sedlák, M.C. Glascock, J.H. Dawson, The heme iron coordination of unfolded ferric and ferrous cytochrome c in neutral and acidic urea solutions. Spectroscopic and electrochemical studies, Biochim. Biophys. Acta 1703 (2004) 31–41.
[32] A. Muga, H.H. Mantsch, W.K. Surewicz, Membrane binding induces destabilization of cytochrome c structure, Biochemistry 30 (1991) 7219–7224.
[33] E. Sedlák, M. Antalík, J. Bágel'ová, M. Fedurco, Interaction of ferricytochrome c with polyanion Nafion, Biochim. Biophys. Acta 1319 (1997) 258–266.
[34] E. Sedlák, M. Antalík, Coulombic and noncoulombic effect of polyanions on cytochrome c structure, Biopolymers 46 (1998) 145–154.
[35] A.M. Davies, J.G. Guillemette, M. Smith, C. Greenwood, A.G.P. Thurgood, A.G. Mauk, G.R. Moore, Redesign of the interior hydrophilic region of mitochondrial cytochrome c by site-directed mutagenesis, Biochemistry 32 (1993) 5431–5435.
[36] D.W. Urry, The heme chromophore in the ultraviolet, J. Biol. Chem. 242 (1967) 4441–4448.
[37] T.Y. Tsong, The Trp-59 fluorescence of ferricytochrome *c* as a sensitive measure of the over-all protein conformation, J. Biol. Chem. 249 (1974) 1988–1990.
[38] M.-F. Jeng, S.W. Englander, Stable submolecular folding units in a non-compact form of cytochrome c, J. Mol. Biol. 221 (1991) 1045–1061.
[39] G.W. Bushnell, G.V. Louie, G.D. Brayer, High-resolution 3-dimensional structure of horse heart cytochrome c, J. Mol. Biol. 214 (1990) 585–595.
[40] T.Y. Tsong, An acid induced conformational transition of denatured cytochrome c in urea and guanidine hydrochloride solutions, Biochemistry 14 (1975) 1542–1547.
[41] T.Y. Tsong, Ferricytochrome c chain folding measured by the energy transfer of tryptophan 59 to the heme group, Biochemistry 15 (1976) 5467–5473.
[42] T.R. Sosnick, L. Mayne, S.W. Englander, Molecular collapse: the rate-limiting step in two-state cytochrome c folding, Proteins Struct. Funct. Genet. 24 (1996) 413–426.
[43] P.L. Privalov, A.I. Dragan, Microcalorimetry of biological macromolecules, Biophys. Chem. 126 (2007) 16–24.
[44] C.M. Johnson, Differential scanning calorimetry as a tool for protein folding and stability, Arch. Biochem. Biophys. 531 (2013) 100–109.
[45] R.M.C. Dawson, D.C. Elliott, W.H. Elliott, K.M. Jones, Data for Biochemical Research, 3rd ed. Oxford University Press, 1986. 436.
[46] J.A. Rupley, Horse heart cytochrome c. spectrophotometric titration and viscosity changes in alkaline solution, Biochemistry 3 (1964) 1648–1650.
[47] D. Fedunová, M. Antalík, Prevention of thermal induced aggregation of cytochrome c at isoelectric pH values by polyanions, Biotechnol. Bioeng. 93 (2006) 485–493.
[48] M. Bánó, J. Marek, M. Stupák, Hydrodynamic parameters of hydrated macromolecules: Monte-Carlo calculation, Phys. Chem. Chem. Phys. 6 (2004) 2358–2363.
[49] Y.G. Thomas, R.A. Goldbeck, D.S. Kliger, Characterization of equilibrium intermediates in denaturant-induced unfolding of ferrous and ferric cytochromes c using magnetic circular dichroism, circular dichroism, and optical absorption spectroscopies, Biopolymers 57 (2000) 29–36.
[50] G.R. Moore, G.W. Pettigrew, Cytochromes C: Evolutionary, Structural and Physicochemical Aspects, Springer-Verlag, Berlin, 1990.
[51] L.L. Pearce, A.L. Gärtner, M. Smith, A.G. Mauk, Mutation-induced perturbation of the cytochrome c alkaline transition, Biochemistry 28 (1989) 3152–3156.
[52] N. Tomášková, R. Varhač, G. Žoldák, L. Olekšáková, D. Sedláková, E. Sedlák, Conformational stability and dynamics of cytochrome c affect its alkaline isomerization, J. Biol. Inorg. Chem. 12 (2007) 257–266.
[53] S.G. Sivakolundu, P.A. Mabrouk, Insights into the alkaline transformation of ferricytochrome c from ^{1}H NMR studies in 30% acetonitrile-water, Protein Sci. 10 (2001) 2291–2300.
[54] K. Muthukrishnan, B.T. Nall, Effective concentrations of amino acid side chains in an unfolded protein, Biochemistry 30 (1991) 4706–4710.
[55] C.M. Jones, E.R. Henry, Y. Hu, C.-K. Chan, S.D. Luck, A. Bhuyan, H. Roder, J. Hofrichter, W.A. Eaton, Fast events in protein folding initiated by nanosecond laser photolysis, Proc. Natl. Acad. Sci. U. S. A. 90 (1993) 11860–11864.
[56] G.A. Elöve, A.K. Bhuyan, H. Roder, Kinetic mechanism of cytochrome c folding: involvement of the heme and its ligands, Biochemistry 33 (1994) 6925–6935.
[57] W. Colón, L.P. Wakem, F. Sherman, H. Roder, Identification of the predominant nonnative histidine ligand in unfolded cytochrome c, Biochemistry 36 (1997) 12535–12541.
[58] M. Hüttemann, P. Pecina, M. Rainbolt, T.H. Sanderson, V.E. Kagan, L. Samavati, J.W. Doan, I. Lee, The multiple functions of cytochrome c and their regulation in life and death decisions of the mammalian cell: from respiration to apoptosis, Mitochondrion 11 (2011) 369–381.
[59] M.O. Pereverzev, T.V. Vygodina, A.A. Konstantinov, V.P. Skulachev, Cytochrome c, an ideal antioxidant, Biochem. Soc. Trans. 31 (2003) 1312–1315.
[60] C. Garrido, L. Galluzzi, M. Brunet, P.E. Puig, C. Didelot, G. Kroemer, Mechanisms of cytochrome c release from mitochondria, Cell Death Differ. 13 (2006) 1423–1433.
[61] E. Sedlák, M. Fabian, N.C. Robinson, A. Musatov, Ferricytochrome c protects mitochondrial cytochrome c oxidase against hydrogen peroxide-induced oxidative damage, Free Radic. Biol. Med. 49 (2010) 1574–1581.

[62] F. Sinibaldi, E. Droghetti, F. Polticelli, M.C. Piro, D. Di Pierro, T. Ferri, G. Smulevich, R. Santucci, The effects of ATP and sodium chloride on the cytochrome c-cardiolipin interaction: the contrasting behavior of the horse heart and yeast proteins, J. Inorg. Biochem. 105 (2011) 1365–1372.
[63] V.E. Bychkova, O.B. Ptitsyn, The molten globule in vitro and in vivo, Chemtracts Biochem. Mol. Biol. 4 (1993) 133–163.
[64] V.E. Bychkova, A.E. Dujsekina, S.I. Klenin, E.I. Tiktopulo, V.N. Uversky, O.B. Ptitsyn, Molten globule-like state of cytochrome c under conditions simulating those near the membrane surface, Biochemistry 35 (1996) 6058–6063.
[65] K.C. Mugnol, R.A. Ando, R.Y. Nagayasu, A. Faljoni-Alario, S. Brochsztain, P.S. Santos, O.R. Nascimento, I.L. Nantes, Spectroscopic, structural, and functional characterization of the alternative low-spin state of horse heart cytochrome c, Biophys. J. 94 (2008) 4066–4077.
[66] R.E. Diederix, M. Ubbink, G.W. Canters, The peroxidase activity of cytochrome c-550 from *Paracoccus versutus*, Eur. J. Biochem. 268 (2001) 4207–4216.
[67] M. Garcia Fernandez, L. Troiano, L. Moretti, M. Nasi, M. Pinti, S. Salvioli, J. Dobrucki, A. Cossarizza, Early changes in intramitochondrial cardiolipin distribution during apoptosis, Cell Growth Differ. 13 (2002) 449–455.
[68] V.E. Kagan, V.A. Tyurin, J. Jiang, Y.Y. Tyurina, V.B. Ritov, A.A. Amoscato, A.N. Osipov, N.A. Belikova, A.A. Kapralov, V. Kini, I.I. Vlasova, Q. Zhao, M. Zou, P. Di, D.A. Svistunenko, I.V. Kurnikov, G.G. Borisenko, Cytochrome c acts as a cardiolipin oxygenase required for release of proapoptotic factors, Nat. Chem. Biol. 1 (2005) 223–232.
[69] L.V. Basova, I.V. Kurnikov, L. Wang, V.B. Ritov, N.A. Belikova, I.I. Vlasova, A.A. Pacheco, D.E. Winnica, J. Peterson, H. Bayir, D.H. Waldeck, V.E. Kagan, Cardiolipin switch in mitochondria: shutting off the reduction of cytochrome c and turning on the peroxidase activity, Biochemistry 46 (2007) 3423–3434.
[70] M. Simon, V. Metzinger-Le Meuth, S. Chevance, O. Delalande, A. Bondon, Versatility of non-native forms of human cytochrome c: pH and micellar concentration dependence, J. Biol. Inorg. Chem. 18 (2013) 27–38.
[71] L. Banci, I. Bertini, A. Rosato, G. Varani, Mitochondrial cytochromes c: a comparative analysis, J. Biol. Inorg. Chem. 4 (1999) 824–837.